Analysis of Waveguide Components using H_0–Curl Hexahedral Edge Elements in MSC/EMAS

J. F. DeFord and P. Saladin
MacNeal–Schwendler Corporation, Electromagnetic Development Branch
4300 W. Brown Deer Rd., Suite 300
Milwaukee, WI 53223

Introduction

The finite element method (see Ref. [1] for a compendium of papers on the applications of the finite element method to electromagnetics) is widely used in low–frequency electromagnetics, where nodal elements are commonly employed to represent the electromagnetic fields or potentials in the simulation volume. In high–frequency applications nodal elements suffer from two principal shortcomings: (1) an ineffective representation of perfectly conducting corners, and (2) the requirement of vector component continuity across element boundaries, which is a liability in regions of high field gradients.

Edge elements address the shortcomings of nodal elements by possessing only projection degrees of freedom, and by allowing a discontinuity in the normal components of the fields across element boundaries [2]. MSC/EMAS is a general purpose electromagnetics modeling code that has both nodal and edge element formulations available for use on unstructured meshes containing arbitrary combinations of hexahedra, tetrahedra, and triangular prisms in 3–D. In this paper we focus on the use of the H_0–curl edge element formulation on hexahedra.

H_0–Curl Edge Elements in MSC/EMAS

The general formulation used in MSC/EMAS represents the electromagnetic fields in terms of the electric scalar and magnetic vector potentials. Edge elements do not require the use of the scalar potential because of the allowed discontinuity in the normal components across element boundaries. Therefore, the equations that are satisfied in AC analysis are given by:

$$\nabla \times \frac{1}{\mu} \nabla \times \vec{A} = j\sigma\omega\vec{A} - \epsilon\omega^2\vec{A}$$
$$\omega^2 \nabla \cdot \left(\epsilon\vec{A}\right) = j\omega\nabla \cdot \left(\sigma\vec{A}\right)$$

where ω is the radial frequency, A is the magnetic vector potential, and μ, ε, and σ are the permeability, permittivity, and conductivity, respectively. The electric field and magnetic flux density are related to the vector potential by the expressions

$$\vec{E} = j\omega\vec{A}$$
$$\vec{B} = \nabla \times \vec{A}$$

In effect, when edge elements are used the potential formulation in MSC/EMAS reduces to an electric field formulation.

TH
2E

The distribution of unknowns on an isoparametric hexahedral element is shown in Fig. 1. In this element the tangential fields are uniform along an edge, and are linear functions of the isoparametric coordinates in directions normal to the edge, falling to zero at each of the three corresponding opposite edges. There are no normal components of the vector potential associated with an edge for this element, although there are contributions to a normal field along an edge from adjacent edge projections. See Lee [3] for a detailed discussion on the H_0–curl element.

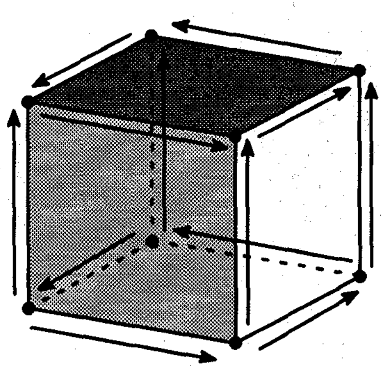

Fig. 1. Distribution of the degrees of freedom on an H_0–curl hexahedral edge element. Unknown components of the vector potential are associated with, and tangential to, element edges.

CH3577-4/95/0000-1207$01.00 © 1995 IEEE

Hybrid–T Junction Application

The hybrid–T junction, also referred to as the "Magic–T", is commonly used in waveguide systems as a power combiner/divider (Fig. 2) [4]. From simple symmetry arguments it may be deduced that power into port 4 is equally divided in–phase into ports 1 and 2. Also, power input into port 3 will be equally divided but 180° out–of–phase at ports 1 and 2. Parameters of interest that may not be determined from simple analytical considerations include the scattering parameters S_{33} and S_{41}, which are important to the overall performance of the device.

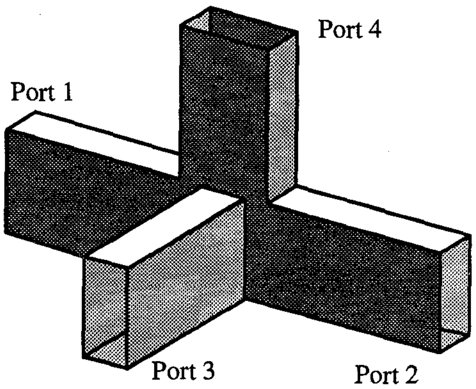

Fig. 2. Hybrid–T waveguide junction.

A solid model representation of the device was generated and meshed using MSC/ARIES (Fig. 3). Note

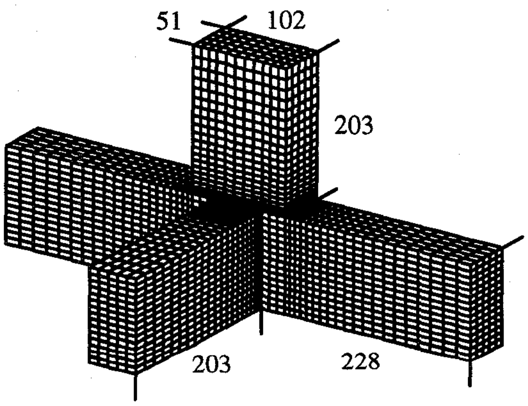

Fig. 3. Hexahedral mesh of hybrid–T waveguide junction. Note element size is graded, resulting in smaller elements near junction. Distances are in millimeters.

that the element size is graded such that the finest mesh is near the junction. This is accomplished by using the mesh biasing feature of the mapped mesher in MSC/ARIES, which allows the user to specify a variation in element dimension along an edge of a logically hexagonal solid region. Mesh refinement of this type is used to improve the accuracy of the results in regions of high field gradients.

Results of several simulations are tabulated in Table 1, and a plot of the magnitude of the real part of the electric field for excitation of the fundamental mode at port 3 is shown in Fig. 4. The tabulated results show good agreement with those developed using a field–matching technique recently published by Alessandri, et al. [5]. The plotted results shown in Fig. 4 exhibit the smooth field vari-

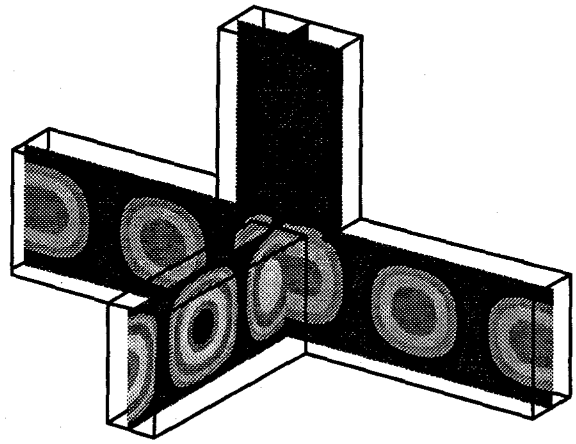

Fig. 4. Magnitude of the real part of the electric field on two orthogonal cut surfaces in hybrid–T waveguide junction.

ation typical of hexahedral elements. A much finer mesh of tetrahedra is necessary to achieve similar local field accuracy, with the commensurate substantial increase in computation time, physical memory, and disk space resources.

Table 1. Comparison of MSC/EMAS and previously published S–parameters for hybrid–T waveguide junction.

S–Parameter	MSC/EMAS Results (dB)	Published Results (dB) [5]
$\lvert S_{11}\rvert$	–18.4	–19.5
$\lvert S_{12}\rvert$	–7.4	–7.3
$\lvert S_{13}\rvert$	–3.7	–3.6
$\lvert S_{41}\rvert$	–4.4	–4.4
$\lvert S_{33}\rvert$	–8.5	–8.5

3–Stub Filter Application

Stub waveguide filters are used to pass and reject certain frequency bands [6]. At a pass band frequency the length of a stub is chosen to be nλ/2 (n an odd integer), which causes its terminating short circuit to be imaged at its base. The use of multiple stubs allows more flexibility in the design, providing for wider pass bands with steeper band edges.

The 3–stub filter we analyzed is shown in Fig. 5,

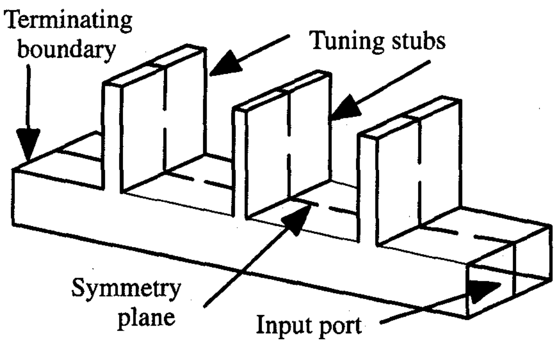

Fig. 5. 3–stub waveguide filter geometry, showing plane of symmetry exploited in simulation.

and the hexahedral mesh for this device is shown in Fig. 6.

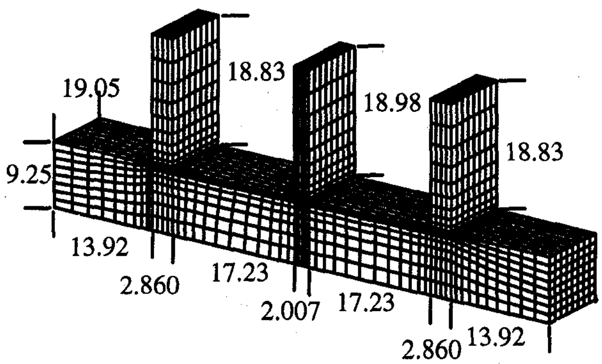

Fig. 6. Hexahedral mesh for 3–stub filter. Note mesh biasing toward stub junctions. All distances are in millimeters.

As in the previous example, the mesh is biased toward the junctions between the guide and the stubs where the field gradients are expected to be large. The $|S_{11}|$ scattering parameter as computed by MSC/EMAS for a range of frequencies spanning both stop bands and pass bands is shown in Fig. 7. Even/odd mode analysis was used to replace a single simulation using the entire mesh (Fig. 6) with two simulations of half the mesh (which uses less computer resources) [7], and a pair of such simulations was done at each frequency. The first of each pair of simulations was done

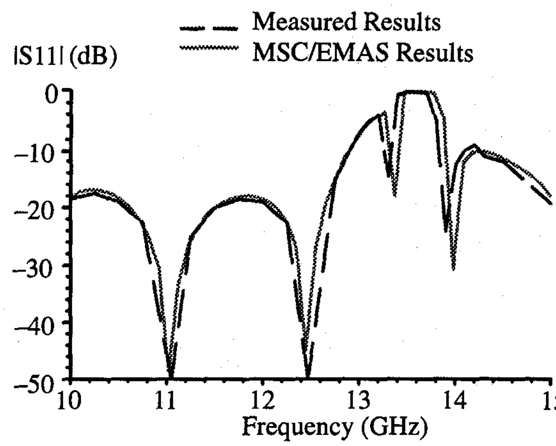

Fig. 7. Comparison of measured and calculated reflection coefficient as measured from input port.

with the mesh terminated at the axial center–point (axial direction is along waveguide axis) with a perfect electric conductor boundary condition, and the second with a perfect magnetic conductor boundary condition. A data point in the plot shown in Fig. 7 was then obtained by averaging the results from the corresponding pair of runs. Also shown is a comparison with experimental measurements on a device of similar geometry. Fig. 8 shows electric field magnitude in the (a) stop band, and (b) pass band. Note that in the pass band the stubs contain $\lambda/2$ wave period, and the field in the guide proceeds unperturbed past the stubs.

Conclusions

Hexahedral H_0–curl edge elements provide the means for highly accurate solutions to the Maxwell equations in the high frequency regime. First order hexahedral elements have proven quite accurate for waveguide component modeling, requiring only a modest amount of mesh refinement near conducting corners where field gradients are highest. Second order (H_1–curl) edge elements have now also been implemented in MSC/EMAS, and testing has shown improved performance in regions of high field gradients.

References

[1] P. P. Silvester and G. Pelosi, editors, *Finite Elements for Wave Electromagnetics*, IEEE Press, New York, 1994.

[2] J. Webb, "Edge elements and what they can do for you," *IEEE Trans. on Magn.*, vol. 29, no. 2, pp. 1460–1465, Mar., 1993.

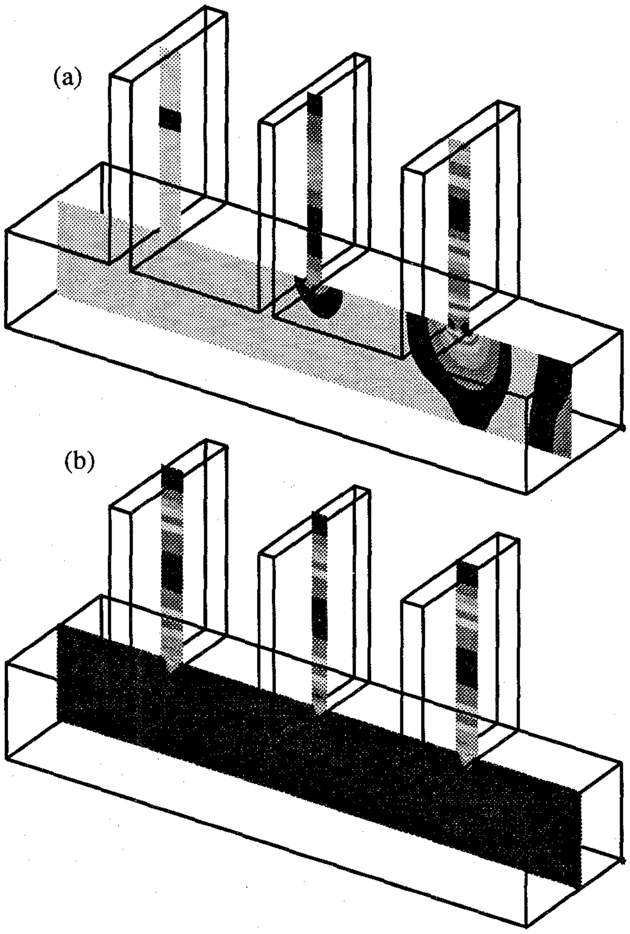

Fig. 8. Magnitude of the electric field at (a) band stop frequency (13.5 GHz), and (b) band pass frequency (11.0 GHz). Fundamental mode is induced at right.

[3] J. Lee, *Finite Element Methods for Modeling Passive Microwave Devices*, Ph. D. dissertation, Carnegie–Mellon University, 1989.

[4] Samuel Y. Liao, "Microwave Devices and Circuits," Prentice Hall, Inc., pp. 95–156.

[5] F. Alessandri, M. Barba, M. Mongiardo, and R. Sorrentino, "Rigorous and efficient analysis of hybrid–T junctions," MWSYM–93, pp. 1447–1450, 1993.

[6] Peter A. Rizzi, Microwave Engineering Passive Circuits, Prentice Hall, Inc., Englewood Cliffs, New Jersey, pp. 454–476.

[7] R. Harrington, *Time–Harmonic Analysis*, McGraw–Hill, New York, pp. 402–406, 1961.